

VIP **Biocatalysis** Very Important PaperHow to cite: *Angew. Chem. Int. Ed.* **2021**, *60*, 13251–13256

International Edition: doi.org/10.1002/anie.202101228

German Edition: doi.org/10.1002/ange.202101228

Stereoselective Directed Cationic Cascades Enabled by Molecular Anchoring in Terpene Cyclases

Andreas Schneider, Philipp Jegl, and Bernhard Hauer*

Abstract: Cascade reactions appeared as a cutting-edge strategy to streamline the assembly of complex structural scaffolds from naturally available precursors in an atom-, as well as time, labor- and cost-efficient way. We herein report a strategy to control cationic cyclization cascades by exploiting the ability of anchoring dynamic substrates in the active site of terpene cyclases via designed hydrogen bonding. Thereby, it is possible to induce “directed” cyclizations in contrast to established “non-stop” cyclizations (99:1) and predestinate cascade termination at otherwise catalytically barely accessible intermediates. As a result, we are able to provide efficient access to naturally widely occurring apocarotenoids, value-added flavors and fragrances in gram-scale by replacing multi-stage synthetic routes to a single step with unprecedented selectivity (> 99.5 % ee) and high yields (up to 89 %).

Introduction

Derived from nature, organocatalytic cascade reactions emerged as an elegant method to substitute classical step-by-step synthetic chemistry.^[1] This sophisticated transformation allows to convert simple starting material into complex molecular frameworks via inter- or intramolecular C-C/C-X coupling accompanied by new formed chiral centers.^[2,3] However, it requires a significant intellectual challenge to master the art of synthesis through cascade reactions (Figure 1 A, left).^[4] The reaction design entails a high level of planning, synthesis knowledge and foresight, as the key to a successful cascade is precise prearrangement of precursors, direction of intermediates and termination control.^[5] In terms of cationic cyclization cascades (or more precisely tandem reactions^[6]), considerable progress has been made towards the initiation and stereocontrol of non-stop cascades.^[7–10] However, for many industrially relevant products those non-stop cascade reactions are disruptive (Figure 1 B, Figure S1).^[11] Furthermore, according to our knowledge, there is

no chemical catalyst described which is able to quench a cationic cascade at a desired intermediary progress in a product- and stereoselective way (= directed cascade) (Figure 1 A).

One of nature’s tools for directing cyclization cascades are terpene cyclases.^[12] These enzymes are able to activate terpenes via pyrophosphate abstraction (class I) or Brønsted acid catalysis (class II) and to control the stereochemical outcome with unprecedented precision by pre-folding of the linear precursor in the enzyme’s active site.^[13] Natural as well as engineered cyclases have already been reported to catalyze such ‘short-circuit’ concerted (but asynchronous) polycyclization cascades and thereby yielding less complex cyclic products.^[14–17] The groups of Hoshino and Peters impressively demonstrated this ability of class I and class II terpene cyclases by introducing amino acids comprising additional steric bulk^[15] or function as catalytic Brønsted bases.^[18] However, these approaches result in unwanted product mixtures^[15] and low isolated yields,^[17] which precludes its industrial application. On the other hand the class II squalene-hopene cyclase from *Alicyclobacillus acidocaldarius* (*AacSHC*), which catalyzes the polycyclization of linear C30 terpene squalene to pentacyclic hopene/hopanol^[19] (Figure S3), has been reported to give reasonable product yields in the biocatalytic production of (–)-Ambrox.^[20] Moreover, our group recently reported the high evolvability and catalytic promiscuity of this enzyme towards several functionalized substrates.^[21]

Given this ability of converting non-natural substrates harboring polar functional groups,^[13] we considered the design of molecular amino acid anchors inside the active site by means of introducing or breaking hydrogen-bonds with the substrate as a concept for controlling cationic cyclization cascades (Figure 1 A, right). This approach would allow to produce industrially relevant cyclic products from natural precursors (Figure 1 B, Figure S1). Molecular anchors are omnipresent core elements in catalysis,^[22,23] computational enzyme design^[24] and materials science^[25] (Figure S2). As a result, the variation of these directing groups by way of rational enzyme design appears promising for directing cascade reactions.

In this paper, we report our studies on carrying out this approach on the *AacSHC* and introduce the stereoselective directed cationic cascade by anchoring functional groups. This alternative strategy to prematurely terminate cyclization cascades allows us to generate valuable chiral apocarotenoids^[27,28] as well as flavor & fragrance compounds with unprecedented selectivity (> 99.5 % ee, > 99.5 % de) and high yields (up to 89 %) from achiral precursors within a single step in water. Furthermore, this approach grants excellent control

[*] A. Schneider, P. Jegl, Prof. Dr. B. Hauer
Institute of Biochemistry and Technical Biochemistry, University of Stuttgart

Allmandring 31, 70569 Stuttgart-Vaihingen (Germany)
E-mail: Bernhard.hauer@itb.uni-stuttgart.de

Supporting information and the ORCID identification number(s) for the author(s) of this article can be found under:
<https://doi.org/10.1002/anie.202101228>.

© 2021 The Authors. Angewandte Chemie International Edition published by Wiley-VCH GmbH. This is an open access article under the terms of the Creative Commons Attribution Non-Commercial NoDerivs License, which permits use and distribution in any medium, provided the original work is properly cited, the use is non-commercial and no modifications or adaptations are made.

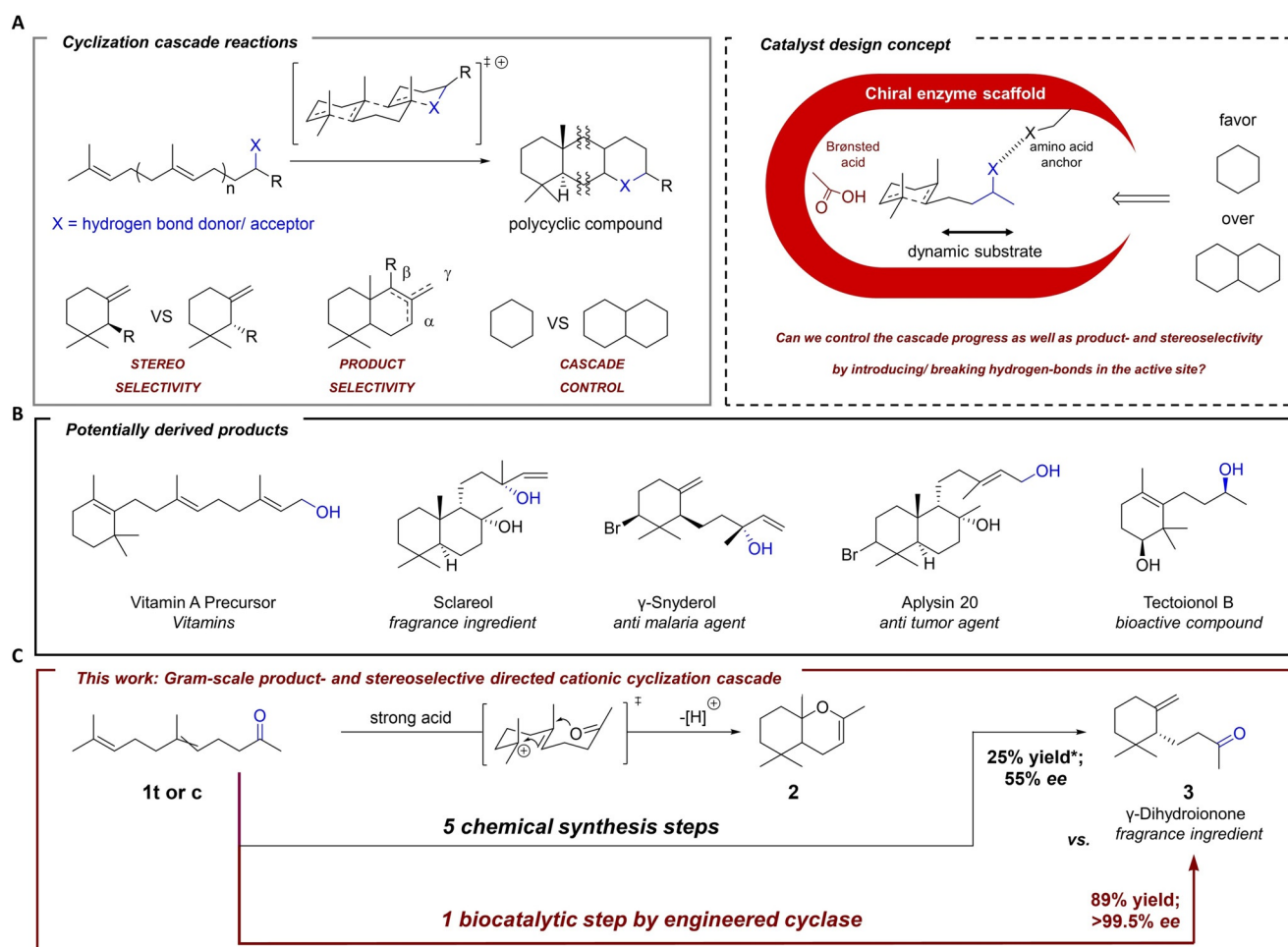


Figure 1. Cationic cyclization cascades and catalyst design concept to control them. (A) Challenges of a cationic cascade (left). The catalyst design concept is based on introducing amino acid anchors in the hydrophobic active site to bind the substrate's polar functional group (blue) at chosen sites consequently directing the cascade reaction. (B) Industrially relevant products, which can be obtained by the demonstrated strategy of anchoring the functional group (blue). (C) Brønsted-acid catalyzed cyclization of geranyl acetone **1t** or **c** results in bicyclic product **2** or requires multi-stage synthesis for monocyclic products **3** (Figure S4)^[26] and this work (red arrow): Gram-scale product- and enantioselective monocyclization of neryl acetone **1c** towards (–)- γ -dihydroionone **3** enabled by hydrogen-bond assisted Brønsted-acid biocatalysis in water. *Given yield of ethylene glycol protected **3**.

of the cascade progress (99:1, monocyclization vs. polycyclization) of functionalized substrates (Figure 1C). Our mechanistic analyses demonstrate how molecular anchors can work in concert to pre-organize substrates in enzymes.

Results and Discussion

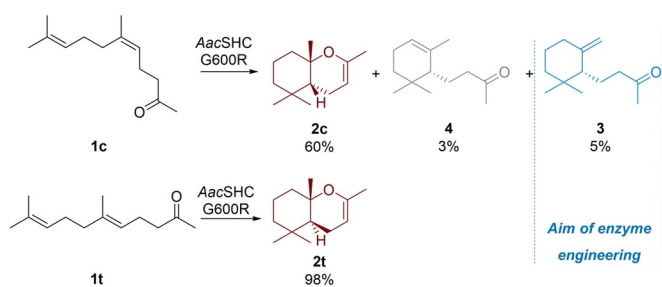
SHC Catalyzed Cyclization of **1t/c** using Variant G600R

In order to find starting activity for potential directed cascade cyclization products, we tested the *E*- and *Z*-isomer of geranyl acetone **1t** (trans)/**c** (cis) (Figure 2) with variant G600R. We chose this approach since we recently discovered the position G600 in AacSHC as a hot spot position for conversion of smaller substrates^[29,30] and the Arginine having bulky but fairly flexible properties. The result of this approach shows that the *E*-isomer **1t** was almost fully converted to a bicyclic product **2t** (Scheme 1, red scaffold). The *Z*-isomer

or neryl acetone **1c** was mainly converted to a bicyclic product **2c** as well as to the monocyclic products α -4 and γ -dihydroionone **3** (Scheme 1, blue scaffold). This means that products **3** and **4** can only be manufactured by way of an engineered enzyme controlling the directed cascade cyclization. Since product **3** is of high demand in the flavor & fragrance industry (Figure S5)—mainly due to its precursor aptitude for most ambra compounds^[31]—we decided to engineer the enzyme towards this compound (for more details see Figure S6).

Engineering Towards Directed Cascade Cyclization of **1c**

The AacSHC-catalyzed cyclization of substrate **1c** potentially results in five products: three monocyclic deprotonation products α -4, β -5 and γ -dihydroionone **3**, the water-addition product **6** of the aforementioned as well as the bicyclic product **2c** (Figure 2A). We challenged the enzyme to direct



Scheme 1. Biotransformation of neryl acetone **1c** and geranyl acetone **1t** with variant G600R. The *E*-isomer **1t** was almost fully converted to the bicyclic product **2t** (red, bottom) and the *Z*-isomer **1c** to bicyclic product **2c** (red, top) as well as monocyclic products **3** (blue) and **4** (grey). Relative conversions are given below the products (for reaction conditions see table S7).

the cascade towards monocyclization, as well as to control this reaction in terms of product- and stereoselectivity. As starting point for the engineering, we decided to pay particular attention to position G600 and saturated this position in order to examine each amino acid in the cyclization reaction. The results disclose that mainly small and polar amino acids drive the monocyclization reaction at position G600. In terms of selectivity, G600T (Figure S7A), that is, variant II, performed best (Figure 2C, D, **II**). Product **5** was not observed at all and the amount of hydration product **6** was negligible (supporting chromatogram G10). In order to rationalize these findings, we performed docking studies of substrate **1c** in the active site of variant II with YASARA.^[32] We are aware of the challenges that arise with docking substrates and homology modelling of terpene cyclases.^[33] However, based on results that show the substrate-bound^[34] and the apo-form^[19] as essentially equal crystal structures and comparing the pre-folding of the squalene-analog aza-squalene bound^[34] (Figure S8) with our docking results, we were confident with our approach. Thereby, we wanted to determine the most probable pre-folding states of neryl acetone **1c** and locate mutational hot spots.

Docking results are depicted in Figure 2B and suggest two major pre-folding states: **Pre-folding state 1** favors bicyclization due to the coordination of the carbonyl moiety by the Y420-hydroxy group. The resulting second carbocation of the cation cascade reaction (Figure 2B, red charge) may interact with one lone-pair of the oxygen and thereby form a covalent bond.^[35] Our experimental results demonstrate how bulky amino acids at position G600 favor this pre-folding state (Figure 2C, G600R and Figure S7A). However, there is a turning point at the size of threonine, where polarity seems to play a more significant role (Figure S7A, G600T and G600V). Earlier studies by Peters and co-workers on terpene cyclases demonstrated that the introduction of threonines or serins as catalytic Brønsted bases adjacent to an intermediary carbocation result in deprotonation and consequently cascade interruption.^[17] However, we assume that this is due to hydrogen-bonding capabilities of polar residues. **Pre-folding state 2** shows the carbonyl moiety hydrogen-bonded by G600T and Y609. Thus, the lone-pairs of the oxygen are facing away from the resulting second carbocation, ultimately

resulting in monocyclic products. Furthermore, steric interaction of the C1-methyl group of the substrate **1c** and the leucine at position 607 can be assumed in this pre-folding state (Figure 2B, dots). Interestingly, the G600T-hydroxy group would be too far away for hydrogen-bonding in this state (Figure 2B, pre-folding state 2), which makes its significance in the catalysis hard to pin down (cf. Mechanistic studies).

Based on the docking results, we performed site-directed mutagenesis at the position L607 and determined amino acids—smaller in size than leucine—as beneficial for the monocyclization reaction (Figure S7B). Remarkably, a combination of variant II with the best mutation L607S did not lead to the best performing double-variant, which we assume is due to earlier reported antagonistic epistatic effects (Table S10).^[36] Instead, variant III (G600T/L607A) turned out to be the best double variant showing almost twice the total turnover number (114 ± 13) compared to II (62 ± 2) and higher selectivity (79%) towards the desired γ -dihydroionone **3** (II: 50%) (Figure 2C,D, **III**). Building on the docking results, we disrupted the hydrogen-bonding at position Y420 with the carbonyl moiety of the substrate **1c** to prevent pre-folding state 1 and thereby bicyclization (Figure 2C, D, **IV**). The resulting variant IV showed 260 ± 4 total turnover with a selectivity of 94% towards the desired product **3**. Bicyclization was reduced to only 2% and the traces of the hydration product were completely eliminated (cf. supporting chromatogram G11). Finally, one further round of site-saturation mutagenesis by employing the 22c-trick^[37] at sites adjacent to position 600 and 607 resulted in variant V with a slightly increased steric bulk at position 306 (A \rightarrow V). The 22c-trick is used in directed evolution of enzymes to reduce the screening effort of protein libraries (for details see ref. [36]). The total turnover number was increased 157-fold compared to the native enzyme and selectivity towards the desired product **3** (Figure 2C, D, **V**) was at 97%. Finally, we performed sulfuric acid-catalyzed cyclization of γ -dihydroionone **3** to obtain enantiopure (+)- α -ambrinol **7** in only two (bio-)synthetic steps compared to the five chemosynthetic steps for enantioenriched material.^[26] Please note that as of now there is no chemical catalyst known which is able to direct the cascade progress (99:1 monocyclization vs. bicyclization) with high product selectivity (97% γ) and excellent enantiocontrol ($>99.5\%$ *ee*) (Figure 2E and Figure S11).

Mechanistic Studies and Substrate Scope

Encouraged by this high selectivity towards the formation of the desired product, we wanted to shed light on the underlying mechanism. Therefore, we performed a systematic deconvolution approach of the variant IV (as the product selectivity was already very high at this point) at positions G600 (A), L607 (B) and Y420 (C). In order to highlight the beneficial hydrogen-bond at position Y609 (D), we further disrupted the hydrogen-bond here (Y \rightarrow F) and combined this mutation with selected deconvolution variants. Figure 3A shows the resulting activities and selectivities of the generated variants compared with variant IV, whereas a letter means a mutation at the above-mentioned position

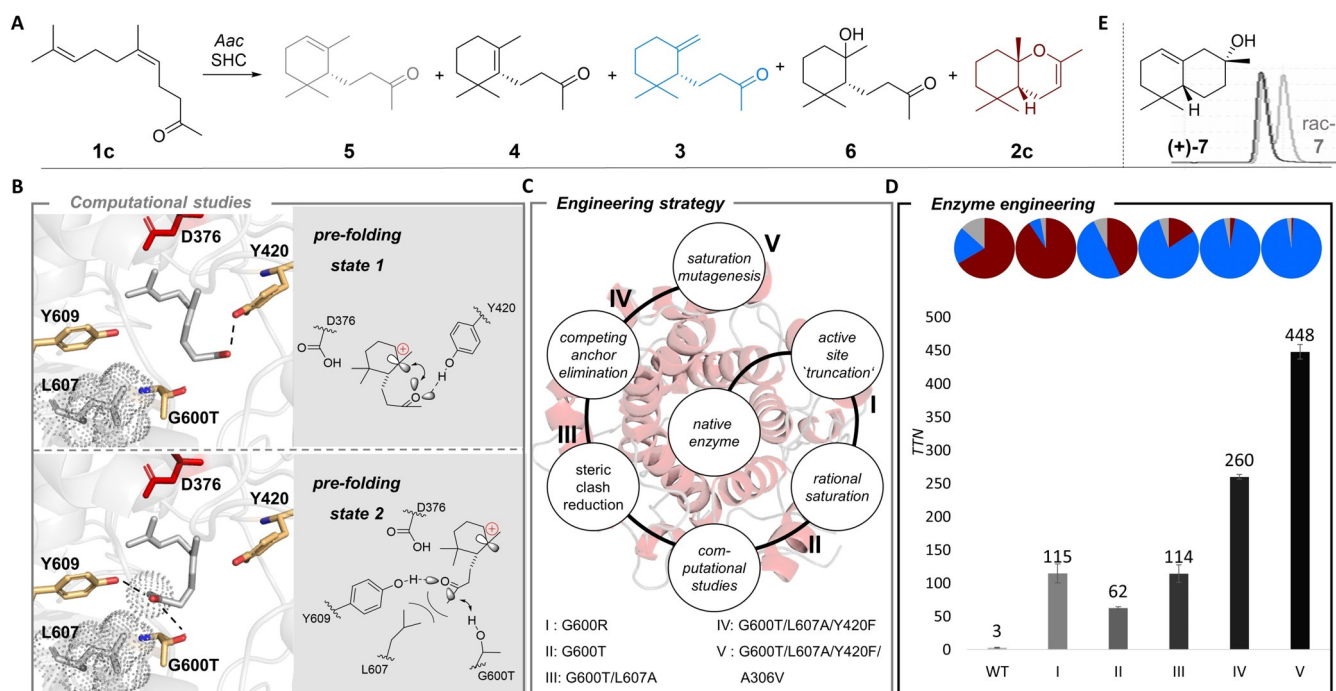


Figure 2. Engineering of AacSHC towards monocyclization of neryl acetone **1c**. (A) AacSHC catalyzed reaction of **1c** may result in five products. Colored scaffolds correspond to the pie charts in (D). (B) Docking of neryl acetone **1c** into the active site of AacSHC G600T (catalytic aspartic acid shown as red sticks; hydrogen-bond donating residues shown as orange sticks, PDB: 2SQC). The results suggest two pre-folding states with similar binding energies ($7.37 \text{ kcal mol}^{-1}$ vs. $7.16 \text{ kcal mol}^{-1}$, see computational methods in supporting information). In pre-folding state 1 the carbonyl moiety is coordinated by the Y420-hydroxy group. After protonation, this allows the resulting second carbocation of **1c** and one lone-pair of the oxygen to interact in the bicyclization of the substrate **2c**. In pre-folding state 2 the carbonyl moiety is flipped towards the residue G600T and Y609 and favors the monocyclization of the substrate **1c** as the interaction of the orbitals is impeded. Steric interaction of the leucine at position 607 and the substrate **1c** is shown in dots. For stereoview see Figure S9. (C) Structure-guided engineering strategy towards directed cationic cascades relied on several stages of rational design and site-directed mutagenesis. (D) Improvement of AacSHC towards monocyclization of neryl acetone **1c** by enzyme engineering. AacSHC variants are compared by their total turnover number (TTN) within 20 h. Selectivities towards mono-/ bicyclic products in (A) are given in pie charts above. Error bars represent the standard deviation of technical triplicates. For details, see Table S11, Figure S10 and Figure S11. (E) Sulfuric acid-catalyzed cyclization of (–)- γ -dihydroionone **3** resulting in enantiopure (+)- α -ambrinol **7** (see Figure S11).

(e.g., variant IV = ABC = G600T/L607A/Y420F). Increasing the steric bulk at position 607 results in 75 % less conversion, albeit selectivity towards the monocyclic product was still high (89 %, Figure 3 A left, blue pie chapter; variant AC). The variant BC (no hydrogen-bond at position 600) showed almost 80 % less conversion and 22 % less selectivity towards the desired product **3**. Variant ABCD (no hydrogen-bond at position 609) lost almost all activity and 50 % of its selectivity towards the monocyclization. The last variant BCD (no hydrogen-bond at position 600 and 609) showed no conversion at all. Furthermore, we performed docking of **1c** in the final variant V and the result with the highest binding energy resembles a similar binding mode as depicted in **pre-folding state 2** (Figure 2 B), but even closer coordinated to the Y609 side chain (Figure 3 A right). Consequently, all the mutational experiments and the computational data led us to the proposed mechanism depicted in Figure 3 B: After the substrate **1c** enters the active site, its carbonyl moiety is loosely coordinated by the threonine at position 600. By this attractive interaction and the created space at position L607 (leucine \rightarrow alanine), the carbonyl moiety flips into the direction of the tyrosine at position 609 for tight binding by a strong hydrogen-bond (cp. IV and ABCD). This hydrogen-

bond mediated conformation allows the highly product- and enantioselective monocyclization of neryl acetone **1c** in one catalytic step. The mediating role of the T600 is emphasized by the variant BC, which still showed some conversion of the substrate with good selectivity (Figure 3 A, variant BC), most likely due to the disabled hydrogen-bond donor at position 420 (tyrosine \rightarrow phenylalanine; Figure 3 A, grey Y420F). By adding the mediating T600, but reducing the size of the hydrogen-bond binding pocket (variant AC), selectivity towards monocyclic product could be improved, whereas activity was lost. The key role of the hydrogen-bond donors as molecular anchors is constituted by the variant BCD that showed no cyclization product at all. (Figure 3 B, variant BCD). These mechanistic hypotheses are strongly supported by the research of Chen et al. wherein the hydrogen-bonding capabilities of water and several functional groups were calculated and experimental binding affinities have been explained.^[38] The authors concluded that tyrosines—compared to other hydrogen-bond donors—are able to bind ketones extremely tight due to matching binding capabilities (cf. supporting text for detailed information).

Subsequently, we investigated the potential of pre-folding via molecular anchoring in the cyclization of analogues

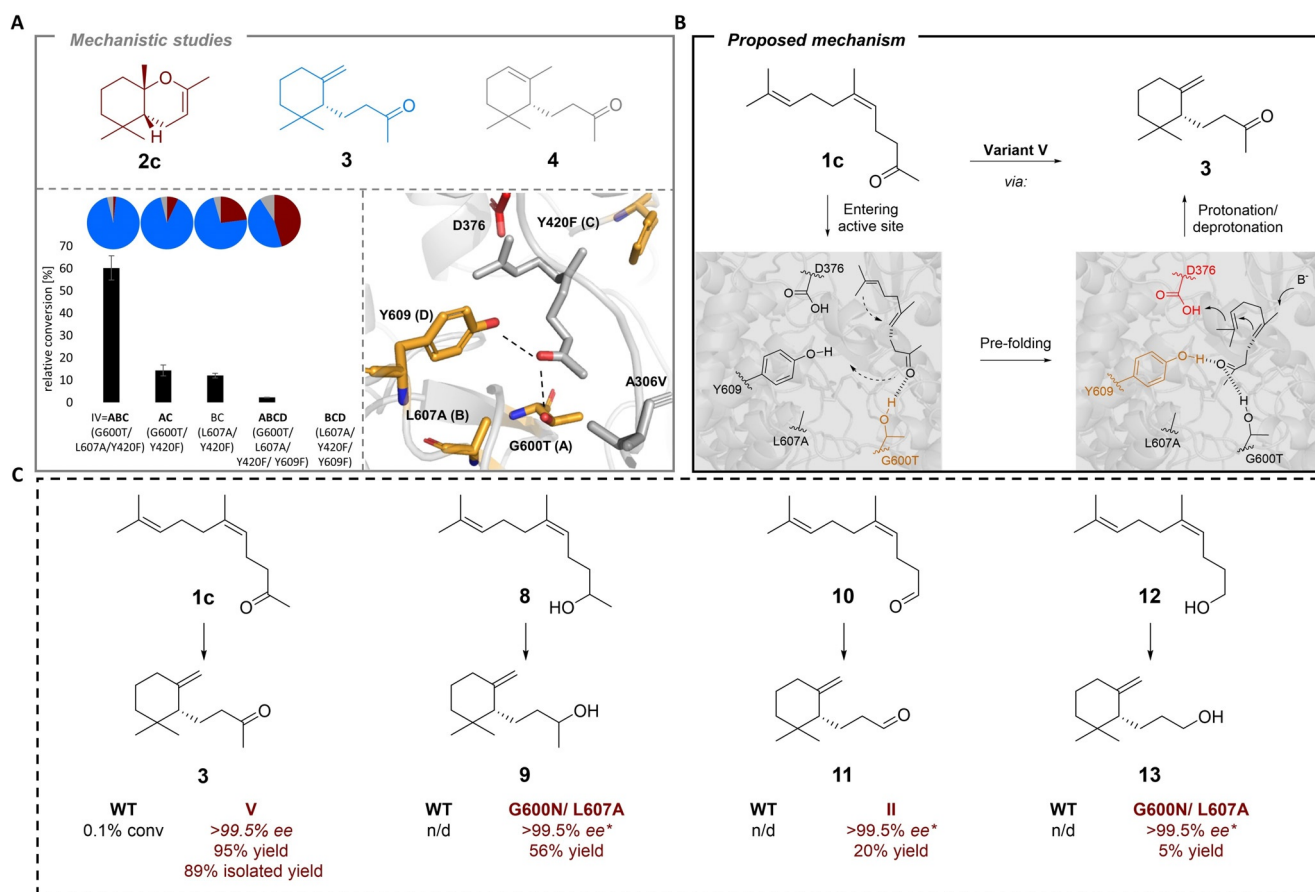


Figure 3. Mechanistic studies on stereoselective monocyclization of neryl acetone **1c** and substrate scope. (A) (Top) Three products of AacSHC catalyzed cyclization of neryl acetone **1c**. Colors correspond to the selectivities below in pie charts (bottom left) Systematic deconvolution variants of IV sorted by relative conversion. Selectivities shown above in pie charts. Variant BCD showed no conversion at all. (bottom right) Docking of substrate **1c** into the active site of V with the best binding energy (protonating aspartic acid shown as red sticks; mutated residues shown as orange sticks. For stereoview see Figure S12. (B) Proposed mechanism for the monocyclization of neryl acetone **1c**. After entering the active site, the substrate's carbonyl moiety is coordinated by the G600T (orange, left) somewhat loosely and mediated to the better coordinating Y609 (orange, right). The substrate's pre-folding results in a monocyclic product after protonation (red)/deprotonation (B^-). (C) Products generated via hydrogen-bond mediated pre-folding in the active site of AacSHC (for reaction conditions see Table S14, S15). *due to enantiopure conversion of Z-substrates.

substrates (Figure 3C). All substrate analogs (**8**, **10**, **12**) of **1c**, varying in the anchor motive (functional group and chain length) were cyclized to monocyclic products (**9**, **12**, **13**) thereby providing access to megastigmane-based natural products, which exhibit great potential in biotechnology and pharmacy.^[39] Interestingly, all four products contained the exocyclic double-bond at the cyclohexane ring which is usually difficult to obtain.^[31] Furthermore, the scalability of this reaction was validated by converting 2 g of neryl acetone **1c** (Figure S13) with the engineered enzyme V expressed in lyophilized whole cells and resuspended in 1 L ddH₂O (+10 mM (2-Hydroxypropyl)-β-cyclodextrin, 0.2% SDS, pH 7.4), with high selectivity (95% γ-**3**; 1% α-**4**; 4% **2c**) towards the desired product **3**. Isolation of the product (89% yield) and subsequent cyclization confirmed enantiopure conversion. It was striking that, when using the *E/Z*-mixture of geranyl acetone **1**, the engineered V converts the *Z*-isomer **1c** prior to the *E*-isomer **1t** (Figure S14), which is another example for cyclization of *Z*-isomers in class II terpene cyclases.^[40] These examples show, first, the general feasibility

of designing molecular anchors for substrate pre-organization and the associated high selectivity. Second, they constitute the scalability of this enzymatic reaction by producing high value products in gram-scale. Third, they demonstrate the importance of fine-tuning molecular anchors, since not every hydrogen-bond has the same power.^[38]

Conclusion

Identification and variation of core elements in catalysis, e.g., cofactors or entrance channels, often lead to unexpected, yet very useful, reaction pathways.^[41,42] We herein focused our engineering on the core element of molecular anchors and highlighted the ability of hydrogen-bond mediated direction of cationic cascades in terpene cyclases. Potential products generated thereby are widely used in the flavor & fragrance^[31] or pharmaceutical industry^[11] and can be produced within a single enzymatic step in water, thus substituting established but cumbersome protection group based chemistry. Going

forward, more computational data in terms of MD simulations and QM/MM calculations have to be generated to undoubtedly confirm the mechanistic details of this precise catalysis.

Acknowledgements

We thank S.C. Hammer, B. M. Nestl, J. Ludwig and K. Schell for fruitful discussions. We thank the Deutsche Forschungsgemeinschaft (DFG HA 1251/6-1) for research funding. B.H. and A.S. designed the overall research project. P.J. performed preliminary experiments, with A.S. providing guidance. A.S. performed docking studies and conducted enzyme engineering. A.S. performed substrate synthesis and substrate scope studies. A.S. performed up-scaling experiments. A. S. performed deconvolution approach. A.S. and B.H. wrote the manuscript. Open access funding enabled and organized by Projekt DEAL.

Conflict of interest

The authors declare no conflict of interest.

Keywords: biocatalysis · Brønsted-acid catalysis · cyclizations · enzymes · sustainable chemistry

- [1] C. Grondal, M. Jeanty, D. Enders, *Nat. Chem.* **2010**, *2*, 167–178.
- [2] R. Ardckhean, D. F. J. Caputo, S. M. Morrow, H. Shi, Y. Xiong, E. A. Anderson, *Chem. Soc. Rev.* **2016**, *45*, 1557–1569.
- [3] U. Wille, *Chem. Rev.* **2013**, *113*, 813–853.
- [4] K. C. Nicolaou, D. J. Edmonds, P. G. Bulger, *Angew. Chem. Int. Ed.* **2006**, *45*, 7134–7186; *Angew. Chem.* **2006**, *118*, 7292–7344.
- [5] K. C. Nicolaou, J. S. Chen, *Chem. Soc. Rev.* **2009**, *38*, 2993–3009.
- [6] F. Rudroff, M. D. Mihovilovic, H. Gröger, R. Snajdrova, H. Iding, U. T. Bornscheuer, *Nat. Catal.* **2018**, *1*, 12–22.
- [7] S. V. Pronin, R. A. Shenvi, *Nat. Chem.* **2012**, *4*, 915–920.
- [8] A. Sakakura, A. Ukai, K. Ishihara, *Nature* **2007**, *445*, 900–903.
- [9] S. Nakamura, K. Ishihara, H. Yamamoto, *J. Am. Chem. Soc.* **2000**, *122*, 8131–8140.
- [10] N. Tsuji, J. L. Kennemur, T. Buyck, S. Lee, S. Prévost, P. S. J. Kaib, D. Bykov, C. Farès, B. List, *Science* **2018**, *359*, 1501–1505.
- [11] S. A. Snyder, D. S. Treitler, A. P. Brucks, *J. Am. Chem. Soc.* **2010**, *132*, 14303–14314.
- [12] D. W. Christianson, *Chem. Rev.* **2017**, *117*, 11570–11648.
- [13] S. C. Hammer, P. O. Syrén, M. Seitz, B. M. Nestl, B. Hauer, *Curr. Opin. Chem. Biol.* **2013**, *17*, 293–300.
- [14] M. Köksal, H. Hu, R. M. Coates, R. J. Peters, D. W. Christianson, *Nat. Chem. Biol.* **2011**, *7*, 431–433.
- [15] T. Hoshino, T. Sato, *Chem. Commun.* **2002**, 291–301.
- [16] P. Moosmann, F. Ecker, S. Leopold-Messer, J. K. B. Cahn, C. L. Dieterich, M. Groll, J. Piel, *Nat. Chem.* **2020**, *12*, 968–972.
- [17] P. R. Wilderman, R. J. Peters, *J. Am. Chem. Soc.* **2007**, *129*, 15736–15737.
- [18] M. Xu, P. R. Wilderman, R. J. Peters, *Proc. Natl. Acad. Sci. USA* **2007**, *104*, 7387–7401.
- [19] K. U. Wendt, A. Lenhart, G. E. Schulz, *J. Mol. Biol.* **1999**, *286*, 175–187.
- [20] E. Eichhorn, E. Locher, S. Guillemer, D. Wahler, L. Fourage, B. Schilling, *Adv. Synth. Catal.* **2018**, *360*, 2339–2351.
- [21] S. C. Hammer, A. Marjanovic, J. M. Dominicus, B. M. Nestl, B. Hauer, *Nat. Chem. Biol.* **2015**, *11*, 121–126.
- [22] X. Huang, B. Wang, Y. Wang, G. Jiang, J. Feng, H. Zhao, *Nature* **2020**, *584*, 69–74.
- [23] Z. Zhang, K. Tanaka, J. Q. Yu, *Nature* **2017**, *543*, 538–542.
- [24] J. B. Siegel, A. Zanghellini, H. M. Lovick, G. Kiss, A. R. Lambert, J. L. St Clair, J. L. Gallaher, D. Hilvert, M. H. Gelb, B. L. Stoddard, K. N. Houk, F. E. Michael, D. Baker, *Science* **2010**, *329*, 309–313.
- [25] M. Mara, Y. Iwakabe, K. Tochigi, H. Sasabe, A. F. Garito, A. Yamada, *Nature* **1990**, *344*, 228–230.
- [26] J. Justicia, A. G. Campañ, B. Bazdi, R. Robles, J. M. Cuerva, J. E. Oltra, *Adv. Synth. Catal.* **2008**, *350*, 571–576.
- [27] S. D. Tetali, *Planta* **2019**, *249*, 1–8.
- [28] E. H. Harrison, L. Quadro, *Annu. Rev. Nutr.* **2018**, *38*, 153–172.
- [29] S. C. Hammer, P.-O. Syrén, B. Hauer, *ChemistrySelect* **2016**, *1*, 3589–3593.
- [30] P. O. Syrén, S. Henche, A. Eichler, B. M. Nestl, B. Hauer, *Curr. Opin. Struct. Biol.* **2016**, *41*, 73–82.
- [31] S. Serra, *Flavour Fragrance J.* **2013**, *28*, 46–52.
- [32] H. Land, M. S. Humble, in *Methods Mol. Biol.*, Humana Press Inc., Totowa, NJ, **2018**, pp. 43–67.
- [33] T. E. O'Brien, S. J. Bertolani, D. J. Tantillo, J. B. Siegel, *Chem. Sci.* **2016**, *7*, 4009–4015.
- [34] D. J. Reinert, G. Balliano, G. E. Schulz, *Chem. Biol.* **2004**, *11*, 121–126.
- [35] A. Krapp, F. M. Bickelhaupt, G. Frenking, *Chem. Eur. J.* **2006**, *12*, 9196–9216.
- [36] M. T. Reetz, *Angew. Chem. Int. Ed.* **2013**, *52*, 2658–2666; *Angew. Chem.* **2013**, *125*, 2720–2729.
- [37] S. Kille, C. G. Acevedo-Rocha, L. P. Parra, Z. G. Zhang, D. J. Opperman, M. T. Reetz, J. P. Acevedo, *ACS Synth. Biol.* **2013**, *2*, 83–92.
- [38] D. Chen, N. Oezguen, P. Urvil, C. Ferguson, S. M. Dann, T. C. Savidge, *Sci. Adv.* **2016**, *2*, e1501240.
- [39] V. F. Cataldo, J. López, M. Cárcamo, E. Agosin, *Appl. Microbiol. Biotechnol.* **2016**, *100*, 5703–5718.
- [40] M. Jia, R. J. Peters, *Org. Biomol. Chem.* **2017**, *15*, 3158–3160.
- [41] Z. C. Litman, Y. Wang, H. Zhao, J. F. Hartwig, *Nature* **2018**, *560*, 355–359.
- [42] A. Gora, J. Brezovsky, J. Damborsky, *Chem. Rev.* **2013**, *113*, 5871–5923.

Manuscript received: January 26, 2021

Revised manuscript received: February 15, 2021

Accepted manuscript online: March 26, 2021

Version of record online: May 6, 2021